

Enhanced Sum Frequency Generation from a Monolayer Adsorbed on a Composite Dielectric/Metal Substrate

Alex G. Lambert, David J. Neivandt,[†] Adam M. Briggs,[‡] Eric W. Usadi,[§] and Paul B. Davies*

Department of Chemistry, University of Cambridge, Lensfield Road, Cambridge CB2 1EW, U.K.

Received: March 21, 2002; In Final Form: July 17, 2002

A composite dielectric/metal substrate, consisting of a thin mica sheet backed with a gold film, has been employed to enhance the intensity of sum frequency vibrational spectroscopy (SFS) signals arising from model monolayers of octadecylsiloxane (ODS) adsorbed at the mica/air interface. In addition to enhanced intensities in comparison to SF spectra of ODS on mica sheets without gold backing, resonant line profiles were found to vary as a function of the thickness of the mica component of the composite substrate. This experimental result concurs with a recent theoretical study of the composite substrate which showed that interference between SF signals arising from the ODS monolayer and from the displaced gold surface results in variations in the resonant phase of the SF vibrational mode. The interference phase/thickness effect has been investigated for several composite samples, each containing a series of steps of well-defined mica thicknesses. A periodic relationship between the mica thickness and the measured interference phase was observed for both the symmetric (r^+) and antisymmetric (r^-) methyl stretching modes of the ODS monolayers. The empirically determined periodicities were 3.3 and 3.1 μm for the r^+ and r^- resonances, respectively. These values agree within error with one of two theoretically predicted periodicities, namely, 3.01 μm . Scatter in the experimental data however is symptomatic of a more complicated interference phase/thickness behavior involving the second shorter theoretically predicted periodicity (162 nm). These experimental observations have been examined in the light of the theoretical model used to simulate the composite substrate. It is concluded that the shorter periodicity component (162 nm) is more susceptible to variations in experimental parameters such as distributions of incident beam angles, nonplanarity of mica, etc. and is partially “averaged out” to leave the less susceptible long periodicity component (3.01 μm) dominant.

Introduction

Infrared-visible sum frequency vibrational spectroscopy (SFS) is a surface-specific technique that yields a molecular-level understanding of the processes of adsorption and reaction at interfaces. The wide range of interfaces and adsorption systems to which SFS has now been applied undoubtedly indicate that the technique has emerged from its technical infancy.^{1–4} It is nevertheless well recognized that the choice of substrate substantially affects the strength of the SF signal generated from the system and, hence, the ease and potential success of subsequent experiments. Of specific interest in this work is the application of SFS to hydrophilic surfaces in order to facilitate the study of adsorption from the liquid phase onto industrially relevant mineral oxide surfaces which are of both fundamental and practical interest. As discussed in detail in a recent publication,⁵ the application of SFS to such substrates is experimentally challenging because dielectric materials such as the mineral oxides do not give rise to a substrate-based SF signal. Thus, although an adsorbed monolayer may in principle still generate a resonant SF signal, the substrate-based coherent interference effect that typically produces a substantial increase in the SF signal is absent. Consequently, the majority of SF

studies employing silica substrates,⁶ for example, use picosecond or faster SF laser systems rather than their nanosecond counterparts, relying on the higher sensitivity of the shorter pulse duration spectrometers to successfully probe the adsorbed film. Although nanosecond SF spectrometers are less sensitive than their pico- and femtosecond counterparts, they still provide a significant contribution to published literature and are valued for their reliability, ease of use, and narrow infrared bandwidth. The few SF studies which have been reported on dielectric substrates using the nanosecond time regime have by necessity resorted to novel experimental configurations for obtaining enhanced signal strengths, such as the total internal reflection geometry employed by Conboy et al.^{7,8} or Yang et al.⁹ In contrast, successful nanosecond SF adsorption studies have been performed on model hydrophobic monolayers formed from self-assembled monolayers of alkanethiols on gold by exploiting the large nonresonant SF signal generated from the gold substrate to amplify the resonant SF signal. In addition, the presence of the gold layer allows the determination of the absolute polar orientation of interfacial species. It is thus possible to conceive of an experimental arrangement in which the substrate signal from a metal such as gold is combined with the resonant signal from a monolayer at a mineral oxide surface to produce an enhanced SF signal from the latter which would in turn be detectable by nanosecond spectrometers. Practically, this would involve using a substrate consisting of one side of a (thin) dielectric surface coated with the monolayer of interest and the reverse side coated with a metal film.

* To whom correspondence should be addressed. Phone: +44 1223 336460. Fax: +44 1223 336362. E-mail: PBD2@cam.ac.uk.

[†] Present address: Department of Chemical Engineering, The University of Maine, Orono, Maine 04469-5737, USA.

[‡] Present address: Lever Faberge, 3 St James's Road, Kingston upon Thames, Surrey KT1 2BA, U.K.

[§] Present address: National Physical Laboratory, Queens Road, Teddington, Middlesex TW11 0LW, U.K.

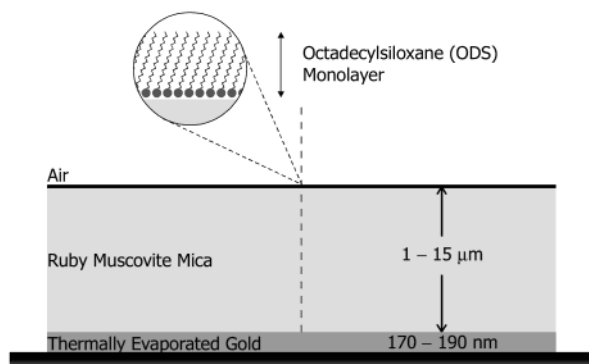


Figure 1. Schematic representation of the composite mica/gold substrate with an inset depicting the ODS monolayer adsorbed at the air/mica interface. The laser beams probing the substrate are omitted for clarity.⁵

In 1997, a feasibility study by Briggs et al.¹⁰ showed that a SF spectrum of a monolayer of octadecylsilane (ODS) adsorbed on mica was readily detectable with a nanosecond spectrometer when the reverse side of the mica was coated with gold (as depicted schematically in Figure 1). This initial study concentrated solely on the signal enhancement properties of the composite mica/gold substrate. An example taken from ref 10 is shown in the Supporting Information and illustrates the significant enhancement achieved. Following the initial feasibility study,¹⁰ the substrate was successfully employed to aid in the development of a reproducible method of forming octadecylsiloxane monolayers on mica.¹¹ However, this further work highlighted a complication with the technique, namely, that the SF spectral line profiles were found to vary as a function of mica thickness. A detailed theoretical study of this effect has recently been completed.⁵ Briefly, it was found that because of the two interfaces present in the composite substrate depicted in Figure 1 the coherent addition of three separate SF signals should be considered: two resonant signals from the air/mica interface and one nonresonant signal from the mica/gold interface. The phase of each of the three SF beams at the point of coherent addition was found to vary independently as a function of mica thickness, with the resulting interference effect generating the observed spectral line-profile variations. Representative calculations were completed to model the line profiles for the symmetric and antisymmetric stretching modes of the terminal methyl group for a well-packed (highly ordered) ODS monolayer adsorbed on mica. For the symmetric stretching mode (ν^+) and its associated Fermi resonance (ν^+_{FR}), it was predicted that the spectral line shape would vary regularly with mica thickness, exhibiting a dominant periodicity of $3.01 \mu\text{m}$ modulated by a very low intensity 162 nm periodicity. In contrast, for the antisymmetric stretching mode (ν^-), the line-shape was calculated to exhibit a dominant periodicity of 162 nm , with an additional underlying component at a periodicity of $3.01 \mu\text{m}$.

The present study tests the theoretical predictions of the composite substrate model by determining the degree of correlation with experimental SF spectra of ODS monolayers on mica, backed by a gold film. The most challenging task in providing quantitative experimental data for verification of the theoretical predictions was determination of the thickness of the dielectric (mica) layer. In principle, an accurate absolute thickness measurement is desirable, but in practice, the inaccuracies inherent in measuring the absolute thickness of a mica sheet were found to be substantial.¹² The method employed in this work, profilometry, resulted in measurements of relative mica thicknesses across stepped pieces of material. Although

only a relative measurement, it has the advantage over an absolute measurement of determining changes in thickness from neighboring layers of material particularly accurately. A detailed picture of the thickness-dependent interference effect has thereby been constructed by correlating the relative thickness data and spectral interference phases from multiple composite substrate samples.

Experimental Section

The mica component of the composite substrate created in this work had to satisfy two criteria. First, it had to be only micrometers in total thickness in order to prevent excessive optical absorption, and second, it had to contain multiple steps of micrometers or less in thickness. A representative experimental substrate is depicted in Figure 2. Substrates were prepared from sheets of ruby muscovite mica (Grade 4, S&J Trading Inc., New York) which were rapidly cleaved and then immediately coated with a layer of gold ($170\text{--}190 \text{ nm}$ in thickness) using a thermal evaporator (Edwards E306A). This resulted in a comparatively thick sheet ($\approx 0.2\text{--}0.5 \text{ mm}$) with a surface consisting of multiple fractures across basal planes and many gold coated steps micrometers in thickness. At this stage, a nonstepped composite sample could be formed by carefully lifting off a single gold coated step from the backing sheet with either a needle, tweezers, or adhesive tape. Alternatively, the stepped samples specifically required in this study could be created by rapidly cleaving a single gold coated step from the backing sheet, thus introducing steps onto the mica side of the composite sample. A densely packed monolayer film of octadecylsiloxane was subsequently formed on the freshly cleaved mica surface from octadecyltrichlorosilane (OTS) using the procedure published by Lambert et al.¹¹ The completed ODS monolayers were characterized by atomic force microscopy (AFM), transmission FTIR, and static advancing contact angle measurements in addition to SFS. Advancing contact angle measurements gave an average value of $108 \pm 2^\circ$ (stable for greater than 15 min). The area occupied per siloxane molecule was determined by transmission FTIR spectroscopy¹³ to be $0.19 \pm 0.03 \text{ nm}^2$, consistent with full monolayer coverage.¹⁴ AFM images from the ODS monolayers indicated a completed film devoid of defects, pinholes, and macroscopic deposits.^{11,12}

SF spectra were recorded on the Cambridge nanosecond spectrometer which has been described previously in the literature.¹⁵ Briefly, a frequency doubled Nd:YAG laser with a pulse duration of 8 ns is used to pump a dye laser, generating red light which is subsequently shifted into the infrared region as it propagates through a multipass Raman cell filled with high-pressure hydrogen. A counter-propagating beam geometry was employed for these experiments with incident visible and infrared beam angles of 60 and 65° to the surface normal, respectively. The SF signal was detected with a photomultiplier tube (9813, Electron Tubes Ltd.) and was analyzed with a digital oscilloscope (LeCroy 9361). Average beam powers at the sample were 15 and 4 mW for the infrared and visible beams, respectively. Spectra were recorded in the ppp (sum frequency, visible, and infrared) laser beam polarization combination. Three spectra of the ODS monolayer were recorded on each mica step, and the spectra were modeled as discussed below to obtain a quantitative description of the line profiles. The modeling procedure was repeated on a number of occasions for each spectrum in order to obtain an indication of the modeling uncertainty, as presented in the tabulated data. Spectra showed no evidence of resonances arising from methylene groups of the ODS hydrocarbon chains (d resonances), indicative of a fully

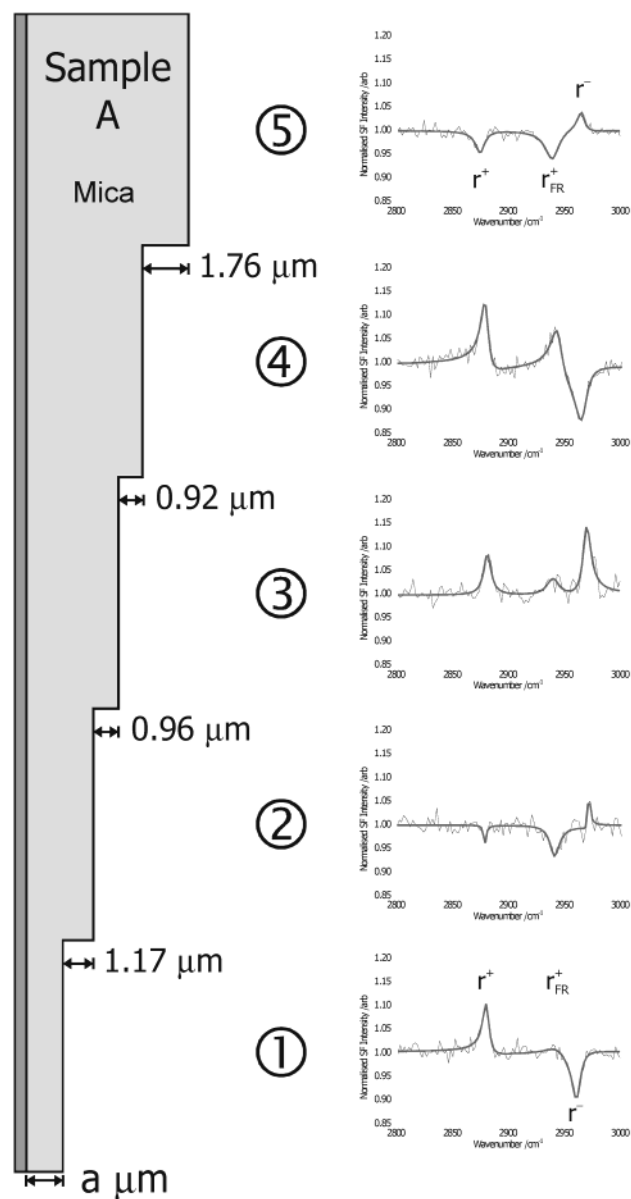


Figure 2. Sample A, a multisteped mica/gold composite substrate represented in schematic form. Profileometric data for each mica step and a typical SF spectrum from each mica plane are included. SF spectra were recorded in the ppp beam polarization combination, at least three spectra were recorded from each mica plane of the sample. Spectra contained only symmetric (r^+ and r^+_{FR}) and antisymmetric (r^-) stretching modes of the terminal methyl group of the ODS alkyl chain. The thick solid line represents the theoretical fit to the experimental data indicated by the light solid line.

trans, highly ordered, conformation. Spectral line profiles analyzed in this work consequently originate purely from the symmetric (r^+ and r^+_{FR}) and antisymmetric (r^-) stretching modes of the terminal methyl group of the ODS hydrocarbon chain. Following spectral acquisition, the step heights of the mica component of the composite substrates were determined with a Sloan Dektak II stylus profileometer. Repetitive measurements showed that the experimental uncertainty in the value of a given step height was $\pm 0.06 \mu\text{m}$. Care was taken to discard samples where there was visual evidence of stepped structure on the gold coated side of the sample, which was inaccessible to the profileometer.

Quantitative analysis of the spectral line profiles observed in the composite substrate SF spectra was fundamental to this work. The spectral curve fitting procedure employed follows

that typically employed in SF spectral analysis¹⁶ and is based on that of Bain et al.¹⁴ The procedure incorporated a Levenberg–Marquardt minimization algorithm and generated values for the resonant band center, fwhm, intensity, and interference phase.¹² The interference phase values for both the r^+ and r^- resonances are denoted as ϵ_r^+ and ϵ_r^- (in degrees), respectively. In our recent publication⁵ describing the theoretical aspects of the composite substrate, the principles of the spectral phase are discussed in detail and the interference phase of a resonant line shape (ϵ) is calculated by analyzing the component phases of each of the contributing SF beams (i.e., eq 28 in ref 5). In the current work, the interference phases of the resonant line shapes are determined by curve fitting the spectral data, and although these empirical values cannot be deconvoluted to provide the phases of the component beams present at the interfaces, they are directly related to the optical interference effects occurring at the composite substrate. Further, this optical interference is not only dependent on the thickness of the mica layer but also on the absolute polar orientation of the adsorbate.^{16,17} Although this additional orientational information is an added advantage of the composite substrate, it has been important in this study to analyze monolayers of consistent polar orientation, thereby isolating purely the mica thickness dependent interference effect.

Results

Seven mica samples each of which exhibited a range of steps of varying thickness were investigated. Sample A contained five mica steps, and a representative spectrum from each of the steps is shown in Figure 2, along with its profileometric height. Only spectra with the ppp laser polarization were obtained as the signal enhancement was found to be significantly greater than for other polarization combinations (ppp generates a stronger SF response from a gold substrate than other polarization combinations). Note that the existence of resonant “dips” (resonances below the baseline) confirms that a coherent interference effect occurs between the multiple SF sources. Indeed, it is clear that there are striking variations in both the phase and intensity of the three methyl resonances, r^+ (2878 cm^{-1}), r^+_{FR} (2940 cm^{-1}), and r^- (2966 cm^{-1}). The ODS film characterization experiments described previously indicate that a well-ordered, complete, ODS monolayer exists uniformly across the sample surface. The observed variations in spectral line shape and intensity must therefore arise from the mica thickness dependent interference effect. A second feature of the spectra is that they appear largely as either peaks or dips, and resonances exhibiting a first derivative or “differential” line-profile are much less in evidence.

The spectra of Figure 2 may be analyzed to provide resonant phase results as a function of mica thickness. The analysis method employed is based upon the assumption that if a periodic interference effect exists then the periodicity will be constant from sample to sample. A corollary of this assumption is that if periodic behavior is absent or if the periodicity is not constant, i.e., it changes with mica thickness, then an overall correlation of phase and mica thickness across samples will not be identified. Figure 3a is a plot of the r^+ interference phase (ϵ_r^+) versus mica thickness for the five steps of sample A. Because profileometry provides only relative mica thickness data, a means of calculating quasiabsolute mica thickness values must be defined. This is achieved by applying a sample specific offset to each set of relative thickness values. The value of the offset is chosen to be the absolute thickness of the mica layer of the thinnest mica plane, for sample A, denoted “ a ”. Thus, for sample A, the first two mica planes are “ $a \mu\text{m}$ ” and “ $a +$

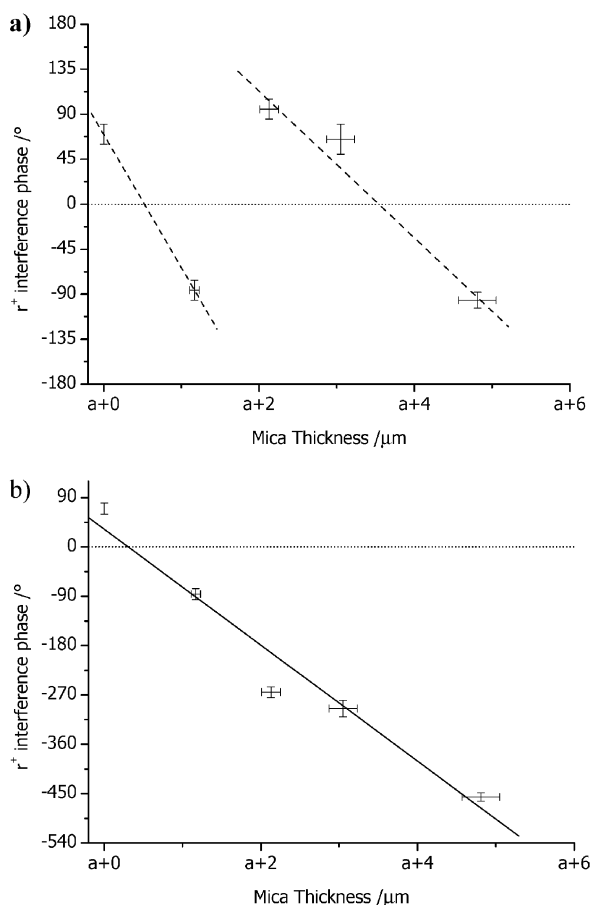


Figure 3. Interference phase of the r^+ vibrational mode of the spectra shown in Figure 2 versus the absolute mica thickness. Uncertainties in the thickness and phase are shown as error bars in the x and y axes, respectively. (a) The phase values plotted are an average of those output directly from the spectral modeling procedure. The dashed lines are guides to the eye and indicate that two periodicity gradients are present in the data. A phase discontinuity is evident at approximately $a + 2 \mu\text{m}$. (b) A 360° phase shift has been applied to the phase data of part a to eliminate the discontinuity and generate an interference phase/thickness plot exhibiting a linear trend. The solid line is a least-squares fit with a gradient of $-106^\circ/\mu\text{m}$ and a periodicity of $3.4 \mu\text{m}$.

$1.17 \mu\text{m}$ in thickness. It is evident from the periodic nature of Figure 3a that an interference phase/thickness effect exists but that there is a discontinuity in the data for thicknesses less than $a + 2 \mu\text{m}$ and greater than $a + 2 \mu\text{m}$. This is a consequence of the curve fitting procedure which provides line-profile interference phases (ϵ_r^+ , ϵ_r^-) bounded by $\pm 180^\circ$. It is therefore necessary to offset the modeled phase results by 360° (or multiples thereof) when a discontinuity is evident in the interference phase/thickness plot for a subset of the data. This procedure has been implemented for the data of sample A, and the resultant plot is given in Figure 3b. The linear nature of the data points confirms the validity of the approach, and a linear least-squares fit yields an r^+ periodicity of $3.4 \pm 0.2 \mu\text{m}$.

r^+ Methyl Vibrational Mode. Each of the seven stepped mica samples considered in this work was analyzed with respect to the interference phase of the r^+ resonance as described above for sample A. In all cases, a trend of decreasing phase with increasing mica thickness was observed, comparable to that evident in Figure 3b. Linear least-squares fitting of the plots resulted in the data collected in Table 1. The calculated periodicity value for each sample was weighted by the number of steps present and averaged to yield a value of $3.3 \mu\text{m}$ with 95% confidence limits of 2.8 and $4.1 \mu\text{m}$ (note that because of

the reciprocal relationship between the least squares linear gradient and the periodicity, the periodicity value does not lie equally between the confidence limits). It is instructive to combine the data from the multiple samples onto a single plot based on absolute mica thickness. To achieve this, the value of the thickness offset applied to the relative thickness data for each sample (A to G) required determination. The sample specific thickness offset was calculated by relating the phase of the spectrum at $0 \mu\text{m}$ relative thickness to a periodicity of $3.3 \mu\text{m}$. At zero absolute thickness, the r^+ interference phase is assumed to be 90° , the value empirically determined for a monolayer adsorbed directly on gold.¹⁶ Thus, for spectrum 1 of sample A, the r^+ interference phase of 70° corresponds to an absolute mica thickness of $0.16 \mu\text{m}$. The value of " a ", the thickness offset for sample A, is therefore set to $0.16 \mu\text{m}$ (or more strictly, $a = 0.16 \mu\text{m}$ plus any multiple of $3.3 \mu\text{m}$). Having determined the sample specific thickness offset from the first spectrum of each sample, the absolute thicknesses for the subsequent mica planes are determined using the profilometry relationships summarized in Table 1. It should be noted that this process uses only the mean value of the periodicity, and the 95% confidence limits are not incorporated into the absolute thickness calculation. Figure 4a is a plot of r^+ interference phase versus absolute mica thickness for all 26 steps of the seven composite substrate samples. Note that Figure 4a employs the original, rather than the 360° , offset interference phase values. Although a number of points deviate significantly from the average periodicity, nearly all lie within the confidence limits, and it is clear that a general trend in the data has been successfully identified. Nevertheless, it is evident from Figures 3b and 4a that for several individual data points the deviation from the determined periodicity trend exceeds the error limits. As described above, these error limits were calculated from multiple profilometry measurements and numerous fittings of spectra for each mica plane, as such they are believed to be a true interpretation of the experimental errors. Although it is appreciated that care must be taken when drawing conclusions from only 26 data points, it is believed that the observed deviation in Figure 4a indicates an additional subtlety in the experimental phase behavior, the origin of which is discussed in more detail later.

r^- Methyl Vibrational Mode. The method employed to analyze the r^- vibrational resonance was identical to that detailed above for the r^+ mode. A linear interference phase/thickness relationship was again evident in the data. The profilometry results, interference phases, and periodicities are presented in Table 2. The weighted average periodicity was calculated to be $3.1 \mu\text{m}$ with 95% confidence limits of 2.3 and $4.7 \mu\text{m}$. The uncertainty in the r^- interference phase determined for an individual spectrum is typically larger than that of the r^+ resonance, principally because the r^- line profile is convoluted with that of the r^+_{FR} . Although the increased uncertainty is included in the error estimates, the standard deviation of the r^- data points from the calculated periodicity is substantially greater than that for the r^+ resonance and is beyond what may be directly attributable to the errors considered. A plot of the r^- interference phase versus absolute mica thickness is given in Figure 4b and was calculated in an identical manner to that for the r^+ data. The wider deviation of the r^- data from the identified periodicity is clearly evident and is discussed below.

Discussion

The spectra presented clearly demonstrate that the multiple SF signals arising from the two interfaces of the composite

TABLE 1: Numerical Interference Phase/Mica Thickness Results for the r^+ Vibrational Resonance (Uncertainties Given in Parentheses)

| sample ID | profileometry thickness (μm) | r^+ interference phase ($^\circ$) | n360 $^\circ$ offset | final phase ($^\circ$) | least squares linear gradient ($^\circ/\mu\text{m}$) |
|-------------------|---|---------------------------------------|----------------------|--------------------------|--|
| A1 | <i>a</i> | 70 (8) | 0 | 70 | |
| A2 | <i>a</i> + 1.17 (0.06) | -86 (15) | 0 | -86 | |
| A3 | <i>a</i> + 2.13 (0.12) | 95 (10) | 1 | -265 | |
| A4 | <i>a</i> + 3.05 (0.18) | 65 (10) | 1 | -295 | |
| A5 | <i>a</i> + 4.81 (0.24) | -96 (10) | 1 | -456 | -108 (13) |
| B1 | <i>b</i> | -118 (20) | 0 | -118 | |
| B2 | <i>b</i> + 0.24 (0.06) | -135 (20) | 0 | -135 | |
| B3 | <i>b</i> + 2.20 (0.12) | -74 (8) | 1 | -295 | -147 (8) |
| C1 | <i>c</i> | 73 (10) | 0 | 73 | |
| C2 | <i>c</i> + 0.17 (0.06) | 57 (10) | 0 | 57 | |
| C3 | <i>c</i> + 3.97 (0.12) | 86 (10) | 1 | -274 | |
| C4 | <i>c</i> + 7.09 (0.18) | 73 (5) | 2 | -647 | |
| C5 | <i>c</i> + 20.53 (0.24) | -101 (10) | 5 | -1901 | -96 (2) |
| D1 | <i>d</i> | -128 (20) | 0 | -128 | |
| D2 | <i>d</i> + 0.93 (0.06) | -162 (20) | 0 | -162 | |
| D3 | <i>d</i> + 3.53 (0.12) | -112 (10) | 1 | -472 | -102 (17) |
| E1 | <i>e</i> | -89 (10) | 0 | -89 | |
| E2 | <i>e</i> + 1.25 (0.06) | 103 (15) | 1 | -257 | -134 |
| F1 | <i>f</i> | 74 (15) | 0 | 74 | |
| F2 | <i>f</i> + 0.04 (0.06) | 82 (10) | 0 | 82 | |
| F3 | <i>f</i> + 0.91 (0.12) | -55 (25) | 0 | -55 | |
| F4 | <i>f</i> + 1.47 (0.18) | -87 (10) | 0 | -87 | -120 (16) |
| G1 | <i>g</i> | 75 (8) | 0 | 75 | |
| G2 | <i>g</i> + 0.29 (0.06) | -93 (15) | 0 | -93 | |
| G3 | <i>g</i> + 3.67 (0.12) | 60 (15) | 1 | -300 | |
| G4 | <i>g</i> + 7.46 (0.18) | 70 (7) | 2 | -650 | -88 (12) |
| weighted average: | | | | | -110 (11) |

substrate interfere coherently, with subsequent amplification of resonant SF signals originating from the monolayer adsorbed at the mica surface. As a consequence, it has been possible to obtain spectra with large signal-to-noise ratios using a nano-second spectrometer. The interference phase evident in the spectral line shapes is dependent on both the absolute polar orientation of the molecules at the interface and any mica thickness effect. By analyzing multiple samples with similar molecular orientation, it has been possible to identify a periodic interference phase/thickness effect for both the r^+ and r^- resonances of the ODS monolayer. Furthermore, correlation between data from different samples has been observed, leading to the conclusion that the determined periodicities are invariant with mica thickness over the range investigated (approximately 1 to 15 μm). The periodicity of the interference phase/thickness effect for the r^+ and r^- vibrational modes has been determined to be 3.3 and 3.1 μm , respectively. Considering the confidence limits of the data, it may be concluded that both vibrational modes exhibit an identical phase behavior. However, for the r^- results (and to a lesser degree the r^+ data), a significant number of data points deviate from the identified periodicity to an extent that is greater than can be attributed to errors arising either from the modeled interference phase or relative thickness determinations. This raises the possibility that the assumption of a single periodicity, although suggested from the method of analysis adopted, may not account for the finer details of the interference phase/thickness behavior. Consideration of the r^+ and r^- phases present in a single sample further challenges the assumption of a single dominant phase. For example, at zero mica thickness (corresponding to a monolayer adsorbed directly on gold), it is commonly accepted¹⁶ that the r^+ and r^- resonances exhibit an identical interference phase (ϵ_r^+ and ϵ_r^- both equal 90° , Figure 4, parts a and b). Having determined that the r^+ and r^- periodicities are at least closely similar, it is therefore contradictory to observe in a single sample r^+ and r^- resonances with almost opposing phases at a given mica thickness, for example, Figure 2, spectra 4 and 5. This contradiction may be accounted

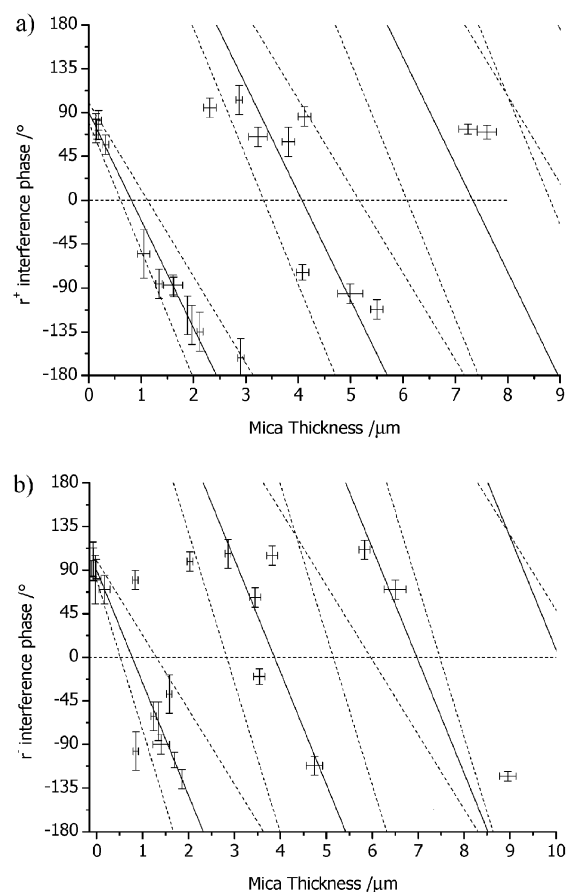


Figure 4. Interference phase as a function of absolute mica thickness for (a) the r^+ vibrational mode and (b) the r^- vibrational mode. The solid lines represent the interference phase/thickness periodicity calculated using a weighted average of the data from the seven composite samples. The dotted lines represent the 95% confidence limits of the periodicity value.

TABLE 2: Numerical Interference Phase/Mica Thickness Results for the r^- Vibrational Resonance (Uncertainties Given in Parentheses)

| sample ID | profileometry thickness (μm) | r^- interference phase ($^\circ$) | n360 $^\circ$ offset | final phase ($^\circ$) | least squares linear gradient ($^\circ/\mu\text{m}$) |
|-----------|---|---------------------------------------|----------------------|--------------------------|--|
| A1 | <i>a</i> | -106 (10) | 0 | -106 | |
| A2 | <i>a</i> + 1.17 (0.06) | 107 (30) | 1 | -253 | |
| A3 | <i>a</i> + 2.13 (0.12) | 105 (10) | 1 | -255 | |
| A4 | <i>a</i> + 3.05 (0.18) | -112 (15) | 1 | -472 | |
| A5 | <i>a</i> + 4.81 (0.24) | 70 (15) | 2 | -650 | -114 (15) |
| B1 | <i>b</i> | -66 (15) | 0 | -66 | |
| B2 | <i>b</i> + 0.24 (0.06) | -38 (25) | 0 | -38 | |
| B3 | <i>b</i> + 2.20 (0.12) | -20 (25) | 1 | -380 | -155 (27) |
| C1 | <i>c</i> | -126 (20) | 0 | -126 | |
| C2 | <i>c</i> + 0.17 (0.06) | 99 (10) | 0 | 99 | |
| C3 | <i>c</i> + 3.97 (0.12) | 111 (25) | 1 | -249 | |
| C4 | <i>c</i> + 7.09 (0.18) | -123 (10) | 2 | -843 | |
| C5 | <i>c</i> + 20.53 (0.24) | -156 (20) | 5 | -1956 | -97 (9) |
| D1 | <i>d</i> | 99 (20) | 0 | 99 | |
| D2 | <i>d</i> + 0.93 (0.06) | -97 (20) | 0 | -97 | |
| D3 | <i>d</i> + 3.53 (0.12) | 62 (10) | 1 | -298 | -104.9 (28) |
| E1 | <i>e</i> | 91 (10) | 0 | 91 | |
| E2 | <i>e</i> + 1.25 (0.06) | -61 (20) | 0 | -61 | -122 |
| F1 | <i>f</i> | 98 (15) | 0 | 98 | |
| F2 | <i>f</i> + 0.04 (0.06) | 80 (5) | 0 | 80 | |
| F3 | <i>f</i> + 0.91 (0.12) | 80 (10) | 0 | 80 | |
| F4 | <i>f</i> + 1.47 (0.18) | -90 (10) | 0 | -90 | -104 (48) |
| G1 | <i>g</i> | 92 (10) | 0 | 92 | |
| G2 | <i>g</i> + 0.29 (0.06) | 70 (10) | 0 | 70 | |
| G3 | <i>g</i> + 3.67 (0.12) | -129 (20) | 1 | -489 | |
| G4 | <i>g</i> + 7.46 (0.18) | -157 (20) | 2 | -877 | -133 (11) |
| | | | | weighted average: | -116 (20) |

for if it is recognized that only the dominant periodicity trend has been identified and that deviations from this trend are evidence of a more complex interference phase/thickness behavior. Furthermore, it is noted that the experimental method employed to identify the periodicities favors the isolation of periodicities on the micrometer length scale. The presence of shorter, nanometer scale, periodicities would only be identified with the use of much smaller incremental changes in mica thickness, a methodology that exceeds the practical limits of the technique employed. Hence, in order to test the hypothesis that other periodicities contribute to the phase behavior, it is useful to examine the results of the theoretical modeling presented earlier.⁵

The principle conclusions of the theoretical modeling study were that periodic interference phase/thickness effects should exist in SF spectra recorded employing the composite substrate and that the periodicities should be invariant with mica thickness. Further, the analysis showed that two distinct periodicities, namely, 3.01 μm and 162 nm, were present in the interference phase/thickness behavior of both the r^+ and r^- vibrational modes. For the r^+ mode, the 3.01 μm periodicity was shown to be prevalent, although the 162 nm periodicity could not be neglected and introduced a phase deviation from the longer periodicity, as shown in Figure 5a. Although the theoretically predicted deviation is smaller than that observed experimentally, it suggests that a combination of both periodicities may account for the distribution of data points observed in Figure 4a. In contrast to the predictions for the r^+ vibrational mode, theoretical simulations for the r^- resonance indicated that the 162 nm periodicity would dominate over the 3.01 μm periodicity, as shown in Figure 5b. On the micrometer thickness scale considered in this work, the phase behavior indicated by Figure 5b would be observed as a random distribution of data points with no evident periodicity. Clearly, the simulation does not concur with the experimental observation of a dominant periodicity of approximately 3 μm . It may be envisaged however that an increased contribution of the 162 nm component to a

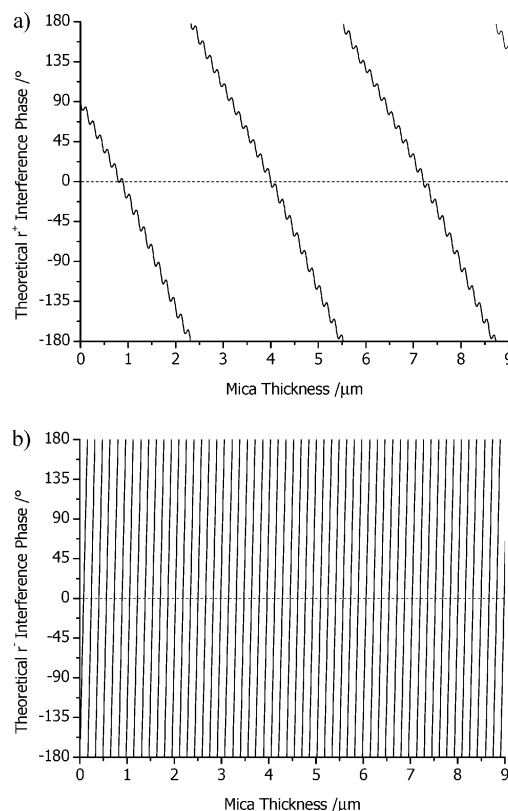


Figure 5. Predicted mica interference phase/thickness behavior for (a) the r^+ symmetric vibrational mode and (b) the r^- antisymmetric vibrational mode. Calculations were completed using the composite substrate theoretical model presented in detail in a recent publication⁵ and employed the equations and constants described therein.

phase prediction similar to that of r^+ resonance would account for the significant deviation of the r^- data points from the approximately 3 μm trend. An explanation for the difference between the observed and predicted phase behavior of the r^-

resonance can be found in an examination of the assumptions on which the theoretical model is based. Importantly, it should be recognized that these assumptions impart a higher degree of order and coherence on the system than exists in practice. This conclusion was reached after examination of how the theoretical simulations responded to variations in modeling parameters such as incident beam angles and refractive indices, as discussed below.

Extension of the theoretical model to take into account realistic angular distributions of the incident laser beams, the birefringent nature of mica, and small variations in the mica thickness results in interference phase/thickness simulations which become an average of a distribution of similar periodicities. Such a distribution affects the 162 nm periodicity more significantly than the $3.01\ \mu\text{m}$ periodicity, thereby reducing its dominance in the r^- resonance results while leaving the underlying $3.01\ \mu\text{m}$ periodicity largely unaffected. A further modeling assumption which affects the relative contributions of the two periodicity components to the interference phase/thickness behavior of the composite substrate is the description of the nonresonant sum frequency signal arising from gold. It should be noted that agreement on a theoretical description of sum frequency generation from metal surfaces is lacking in the literature, and a variety of models of varying complexity are employed. The composite substrate simulation describes sum frequency generation from the gold surface in terms of a beam with equal magnitudes in both the x and z axial directions. An alternative description favoring sum frequency generation in the z direction (i.e., perpendicular to the surface and consistent with plasmon resonance) alters the relative magnitudes of the Cartesian components of the sum frequency signals and leads to the prediction of an increase in the dominance of the 162 nm periodicity for the r^+ resonance and a decrease in dominance for the r^- vibrational modes, coincident with the experimental findings.

Although different descriptions of sum frequency generation from gold, along with experimental distributions of incident angles, refractive indices, and mica thicknesses may be used to account for the differences in the observed and predicted periodicity behavior, two further experimental characteristics must be addressed: the significant resonant intensity variations observed between spectra on a single sample (evident in Figure 2) and the general absence of differential line profiles. Neither of these two empirically observed behaviors were predicted by the theoretical simulations, a fact which may potentially be attributable to the assumption that multiple reflections within the mica layer may be ignored. Classically observed linear thin-film phenomenon are the result of multireflections within a film producing regions of constructive and destructive interference. In a similar manner, it is possible to envisage that the inclusion of linear multireflection effects in the composite substrate model would couple the current phase periodicity predictions with thickness dependent variations in the intensities of the resonant modes. To date, attempts to extend the composite substrate model to incorporate multi reflection effects, while indeed predicting intensity variations, have resulted in predicted phase behaviors which are erratic and are not amenable to description by periodically invariant phenomenon. Such behavior is clearly contrary to that presented in this work.

Conclusions

Sum frequency spectra and corresponding profileometry data presented in this work have allowed an empirical determination of the interference phase/mica thickness phenomenon to be

obtained for both the r^+ and r^- vibrational modes of an aliphatic hydrocarbon chain adsorbed on a composite dielectric/metal substrate. Although the composite substrate model successfully predicts a number of the characteristics of the experimentally observed phase behavior, the relative contributions of the phase components and the intensity variations are less well described. The comparisons discussed in this work have allowed the validity of the assumptions on which the modeling is based to be assessed.

With both theoretical and experimental studies completed, it is valuable to consider the practical application of the composite substrate technique. It is evident that the technique does allow substantial sum frequency signal levels to be obtained from dielectric surfaces previously inaccessible to nanosecond spectrometers (as well as providing high signal levels for shorter pulse duration laser systems). In addition, the interference phase evident in the spectral line-shapes does contain information on the gross molecular orientation, and further work could be completed to isolate the orientational component. The experimental complications of the thickness dependent interference phase phenomenon identified in this work may be avoided by working with samples of a known and constant dielectric thickness. In this manner, samples of $9 \pm 0.2\ \mu\text{m}$ were employed in the ODS adsorption study¹¹ to ensure that all spectra exhibited resonant "peaks" (interference phases of $\approx 90^\circ$) and to minimize resonant intensity fluctuations due to thickness variations between samples. Further, preliminary work has indicated that the symmetric d^+ and d^+_{FR} vibrational modes exhibit an interference phase/thickness phenomena identical to that of the r^+ and r^+_{FR} modes. Comparison of r^+ and d^+ resonance strengths, a commonly employed indication of the degree of conformational order of an adsorbate, may therefore be made. Although obtaining mica of thickness $9 \pm 0.2\ \mu\text{m}$ via cleaving was a laborious task for the ODS experiments described in reference 11, this level of accuracy in the thickness of the dielectric layer is easily achievable by chemical vapor deposition, sputter coating, or spin coating. Current work is concentrating on the magnetron sputter coating of mineral oxide films of known thickness on freshly deposited gold surfaces.

Acknowledgment. The authors thank Dr. P. Fischer for his valuable comments throughout this work. A.G.L. and A.M.B. gratefully acknowledge CASE studentships from the EPSRC held in conjunction with Unilever Research (Port Sunlight Laboratory). A.G.L. also thanks Emmanuel College, Cambridge, for financial support. E.W.U. acknowledges the EPSRC for a Postdoctoral award. D.J.N. thanks the Oppenheimer Fund of the University of Cambridge for a Research Fellowship.

Supporting Information Available: PPP spectra (unnormalized) of an ODS monolayer adsorbed on (a) a pore mica substrate 1 mm thick and (b) a 3.5 micron thick mica substrate with a gold layer on the other surface (Figure 1). This material is available free of charge via the Internet at <http://pubs.acs.org>.

References and Notes

- (1) Buck, M.; Himmelhaus, M. *J. Vac. Sci. Technol. A-Vac. Surf. Films* **2001**, *19*, 2717.
- (2) Richmond, G. L. *Ann. Rev. Phys. Chem.* **2001**, *52*, 357.
- (3) Somorjai, G. A.; McCrea, K. R. *Adv. Catal.* **2000**, *45*, 385.
- (4) Gracias, D. H.; Chen, Z.; Shen, Y. R.; Somorjai, G. A. *Acc. Chem. Res.* **1999**, *32*, 930.
- (5) Lambert, A. G.; Neivandt, D. J.; Briggs, A. M.; Usadi, E. W.; Davies, P. B. *J. Phys. Chem. B* **2002**, *106*, 5461.

- (6) Lagutchev, A. S.; Song, K. J.; Huang, J. Y.; Yang, P. K.; Chuang, T. J. *Chem. Phys.* **1998**, 226, 337.
- (7) Conboy, J. C.; Messmer, M. C.; Richmond, G. L. *J. Phys. Chem.* **1996**, 100, 7617.
- (8) Messmer, M. C.; Conboy, J. C.; Richmond, G. L. *J. Am. Chem. Soc.* **1995**, 117, 8039.
- (9) Yang, Y. J.; Pizzolatto, R. L.; Messmer, M. C. *J. Opt. Soc. Am. B* **2000**, 17, 638.
- (10) Briggs, A. M.; Usadi, E. W.; Davies, P. B. *Abstr. Papers Am. Chem. Soc.* **1997**, 214, 286-PHYS.
- (11) Lambert, A. G.; Neivandt, D. J.; McAloney, R. A.; Davies, P. B. *Langmuir* **2000**, 16, 8377.
- (12) Lambert, A. G. Ph.D. Thesis, University of Cambridge, Cambridge, U.K., 2001.
- (13) Guzonas, D. A.; Hair, M. L.; Tripp, C. P. *Appl. Spectrosc.* **1990**, 44, 290.
- (14) Tidswell, I. M.; Rabedeau, T. A.; Pershan, P. S.; Kosowsky, S. D.; Folkers, J. P.; Whitesides, G. M. *J. Chem. Phys.* **1991**, 95, 2854.
- (15) Bain, C. D.; Davies, P. B.; Ong, T. H.; Ward, R. N.; Brown, M. A. *Langmuir* **1991**, 7, 1563.
- (16) Bain, C. D. *J. Chem. Soc. Faraday Trans.* **1995**, 91, 1281.
- (17) Bain, C. D.; Davies, P. B.; Ong, T. H.; Ward, R. N.; Brown, M. A. *Surface Interface Anal.* **1991**, 17, 529.